

OBSERVATIONS OF EARTHQUAKE MOTIONS, FORCED VIBRATION TESTS
AND THEIR SIMULATION ANALYSES OF PWR-TYPE NUCLEAR STATIONS

T. Utsunomiya, J. Hirose, Y. Watanabe (I)

T. Iwatate (II)

I. Hama, K. Hagio, T. Nishiyama (III)

Presenting Author: I. Hama

SUMMARY

In order to evaluate the vibrational characteristics of reactor buildings of Ikata Nuclear Power Stations, forced vibration tests were carried out and earthquake motions were observed. Using four kinds of analytical models and methods, including those used for the seismic design of the power stations, the dynamic analyses were performed to simulate the vibrational characteristics evaluated from the tests and the observed earthquake motions. The vibrational characteristics obtained by each of the four kinds of simulation analyses agreed well with the characteristics obtained by the forced vibration tests and the observed earthquake motions.

INTRODUCTION

The Ikata Nuclear Power Stations, Unit No.1 and Unit No.2 of the Shikoku Electric Power Co., Inc. are PWR-Type 2-loop plants of 566 MWE each. Unit No.1 has operated since Sept. 1977 and Unit No.2 since March 1982. (Fig.1) The forced vibration tests were performed on the reactor containment facilities (Reactor Building) of Unit No.2 in Feb. 1981 before operation. Three significant earthquakes have been observed at the reactor containment facilities and in the rock under the foundation of Unit No.1 so far; Bungo Channel Earthquake (1977, $M = 4.2$, $\Delta = 21\text{km}$), Suoh-Nada Earthquake (1979, $M = 6.1$, $\Delta = 47\text{ km}$) and Iyonada Earthquake (1981, $M = 5.0$, $\Delta = 15\text{km}$). The Suoh-Nada Earthquake gave larger accelerations than others. This report describes the forced vibration test of Unit No.2, the Suoh-Nada earthquake motion recorded at Unit No.1 and the simulation analyses for them. With the results we have confirmed the adequacy of the seismic designs of structures.

FORCED VIBRATION TESTS OF UNIT NO.2

The reactor containment facilities consist of an outer shield wall (O/S), an inner concrete structure (I/C), and a steel containment vessel (C/V) for each unit. All of the buildings of the facilities were finished and most of the machinery and piping system was set up when the tests were performed. The locations of the measuring points for the beam vibration test for the I/C in Y direction is shown in Fig.2 as an example. The resonance and phase lag curves were obtained at measuring points in the structures.

The resonance and phase lag curves at the operating floor of the I/C in

-
- (I) The Shikoku Electric Power Co., Inc., Takamatsu, Japan
 - (II) Central Research Institute of Electric Power Industry, Chiba, Japan
 - (III) Taisei Corporation, Tokyo, Japan

Y direction is shown in Fig.3 and Fig.4 shows the resonance curves at the measuring points of the I/C were drawn together in Y direction as examples. The first-mode and the second-mode shapes, including the sway-rocking mode of the foundation, is shown in Fig.5. The resonance frequencies and the damping factors of the O/S and the I/C in regard to the beam vibration are shown in Table I along with the resonance frequencies in the seismic design.

Using three kinds of analytical models and methods, including those used for the seismic design of the power stations, the dynamic analyses were performed to simulate the vibrational characteristics evaluated from the tests. (Fig.6) To evaluate the soil-structure interaction we used the following three different models. In these models the same lumped mass model was used for the superstructure. The only difference in the models was the soil model.

- (1) A static swaying-rocking spring model (Fig.7)
The dynamic analysis was performed using the static swaying-rocking spring (Table II) and the modal superposition method with strain-energy modal damping. This model and method were used in the design.
- (2) A dynamic swaying-rocking spring model (Fig.7)
A dynamic swaying-rocking spring was frequency-dependent and was calculated on the base of Dr. H. Tajimi's vibration admittance theory of the soil-structure interaction. The dynamic analysis was performed using Fast Fourier Transform (FFT).
- (3) Three dimensional thin layered element model (Fig.8)
Transfer functions were calculated using the three dimensional thin layered element method developed by Dr. H. Tajimi. The dynamic analysis was performed using FFT.

The strain level of the structures by the forced vibration tests were small and the material properties in this level have to be investigated for the simulation analyses. During the construction of the O/S, eighteen test pieces of the concrete were made. Using these pieces, static and dynamic elastic moduli of concrete in the range of small strain were obtained. The result is shown in Table III and the elastic modulus of concrete was evaluated to be $E_c = 3.7 - 4.0 \times 10^5 \text{ kg/cm}^2$.

The Simulation Analysis (1) (ANAL.1) The first-mode frequencies obtained by the eigen value solution with the elastic modulus of concrete at $E_c = 3.9 \times 10^5 \text{ kg/cm}^2$, are shown in Table I. The response analysis was performed using the analytical shaking force of a sine wave having the amplitude of one ton, and acting at the same place vibrated in the test. The damping factors obtained by the forced vibration tests with the $1/\sqrt{2}$ method were used for the structures. For the sway-rocking spring, the same value of 5% was used as the design. The displacements per unit of the shaking force are shown in Fig.10 and Fig.11 along with the results of the tests.

The Simulation Analysis (2) (ANAL.2) The dynamic sway-rocking spring and the dimensionless frequency ($a_0 = r \cdot \omega / V_s$, ω : circular frequency) are shown in Fig.9. The resonance and phase lag curves were analyzed using the dynamic spring, and are shown in Fig.10 and Fig. 11 compared with the results in tests.

The Simulation Analysis (3) (ANAL.3) The analytical model is shown in Fig. 8. The rock is modeled with ten thin layered elements. The analyzed resonance and phase lag curves are shown in Fig.10 and Fig.11. Fig.10 and Fig.11 show that the results of three kinds of analyses are similar to each other and are nearly equal to those of the tests.

THE SUOH-NADA EARTHQUAKE OBSERVED AT UNIT NO.1

The Suoh-Nada earthquake was observed by the electromagnetic seismographs shown in Fig.12. Twenty-five horizontal and 13 vertical units of seismographs were located at 16 points in the rock under the foundation, on the foundation, and on the structures (O/S, I/C, C/V and A/B).

Fig.13 shows the observed horizontal waves of the Suoh-Nada Earthquake which were measured on top of the main structures and in the rock. This figure shows the propagation of the earthquake motion from the rock to the tops of the structures.

The distribution of the maximum horizontal accelerations of the Suoh-Nada Earthquake are shown in Fig.14.

Using the following four kinds analytical models and methods, those of (1), (2), (3) are used for the simulation analyses for the forced vibration tests of Unit No.2, the dynamic analyses were performed to simulate the vibrational characteristics evaluated from the observed earthquake motions. In these models the same lumped mass model was used for the superstructure.

- (1) A static swaying-rocking spring model (Fig.15, Table IV)
- (2) A dynamic swaying-rocking spring model (Fig.15, Fig.18)
- (3) Three dimensional thin layered element model (Fig.16)
- (4) Finite element model (Fig.17)

The rock is modeled with finite elements and the approximate three dimensional dynamic analysis was performed using FFT.

Fig.19 shows the flow chart of the simulation analysis. The eigen value solution were performed by changing the elastic modulus of concrete parametrically.

The natural frequencies of the analytical model agree with those of the structures obtained from the observed motions when the elastic modulus of concrete is $3.4 - 3.5 \times 10^5 \text{ kg/cm}^2$. Considering that the strain level of the structures was small, these elastic moduli of concrete are appropriate.(TableV) The appropriate damping factors of the I/C, the O/S, and the C/V were obtained by changing them parametrically in time history analyses, where the observed earthquake motion in the rock under the foundation (EL-14.4M) was used.

By $1/\sqrt{2}$ method the average damping factors were $h = 3\%$ (I/C), $h = 3.5\%$ (O/S), and $h = 2\%$ (C/V). In comparing the appropriate damping factors obtained by the simulation analyses, it is found that the C/V and the I/C have the same values as mentioned above but the O/S has 25% lower value than that above.

Fig.20 shows the Fourier spectra of the tops of O/S, I/C, C/V and the foundation obtained by the four kinds of analyses. Fig.21 ~ Fig.24 show the response waves by the analyses.

Four kinds of analyses give very similar Fourier Spectra and response waves to each other and they agree with those of the observed motions.

Conclusion

The vibrational characteristics obtained by each of the four kinds of simulation analyses agreed well with the characteristics obtained by the forced vibration tests and the observed earthquake motions (three kinds). The static swaying-rocking spring model and the modal superposition method which we employed in our seismic designs were simpler for the soil-structure modeling and gave shorter computer running time than the others, and they provided similar accurate results to the others. This model and method in the actual seismic designs is considered to be effective and practical.

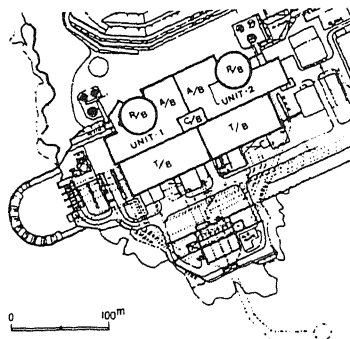


Fig. 1. PLAN OF IKATA NUCLEAR POWER STATION.

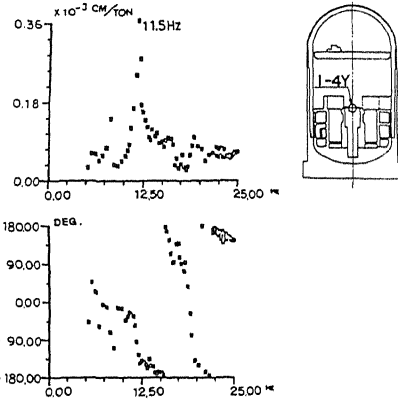


Fig. 3. RESONANCE AND PHASE LAG CURVES OF THE I/C IN Y DIRECTION.

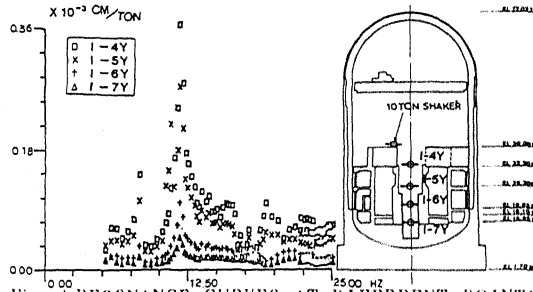


Fig. 4. RESONANCE CURVES AT DIFFERENT POINTS OF THE I/C IN Y DIRECTION.

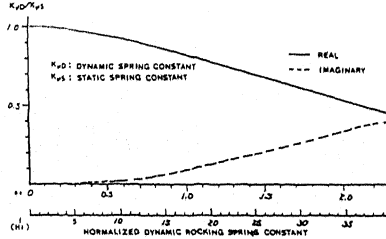


Fig. 9. NORMALIZED DYNAMIC SWAY-ROCKING SPRING

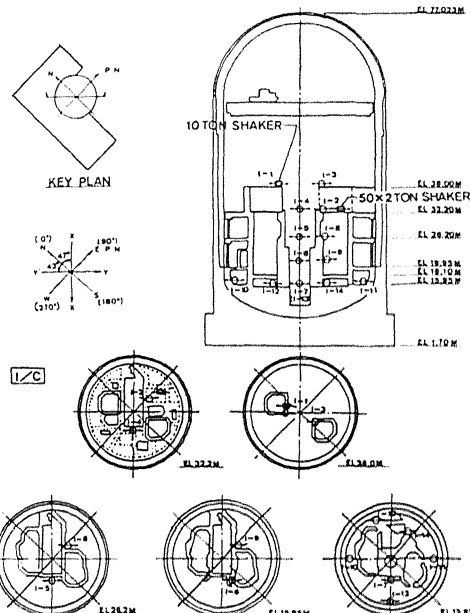


Fig. 2. BEAM VIBRATION TEST FOR THE I/C IN Y DIRECTION.

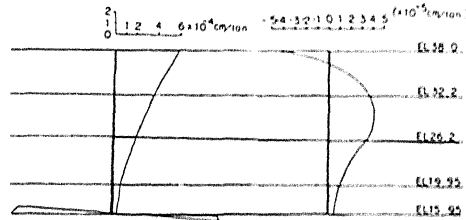
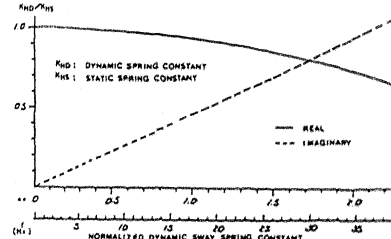


Fig. 5. MODE SHAPES OF THE I/C IN Y DIRECTIONS.

Table 1 FIRST-MODE FREQUENCIES AND DAMPING FACTORS OF THE O/S AND I/C.

| | | FORCED VIBRATION TEST | DESIGN | | | | SIMULATION ANALYSIS | |
|----------------------|-------|-----------------------------|--------------------|------------------|----|---------|---|---------|
| | | | UNCOUPLED MODEL | COUPLED MODEL | | | ($\epsilon = 3.9$ $\times 10^{-4}$ kg/cm ²) | |
| OUTER SHIELD WALL | | 690~718 Hz | 5.5% (50) | 5.5 Hz | 5% | 5.2 Hz | 5% | 6.8 Hz |
| INNER CONCRETE | X-DIR | 15.7~15.9 Hz | 2.8% (5.1) | 11.1 Hz | 5% | 10.5 Hz | 5% | 13.1 Hz |
| | Y-DIR | 11.5~11.8 Hz | 5.1% (5.7) | 9.5 Hz | 5% | 9.1 Hz | 5% | 11.8 Hz |

NOTE: VALUES IN BRACKETS ARE OBTAINED FROM PHASE LAG CURVES.



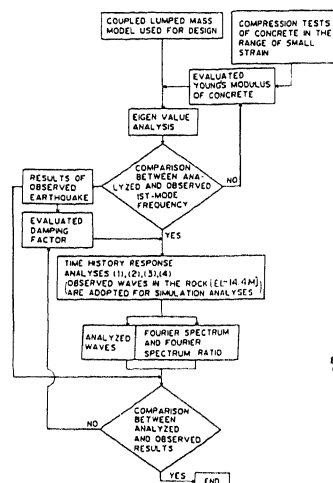


Fig. 19. FLOW CHART OF SIMULATION ANALYSIS

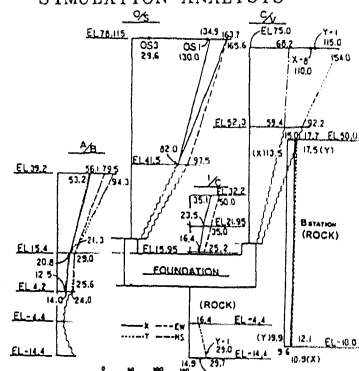


Fig. 14. OBSERVED MAX. ACCELERATION IN HORIZONTAL DIRECTION (SUOH-NADA EARTHQUAKE) (gal)

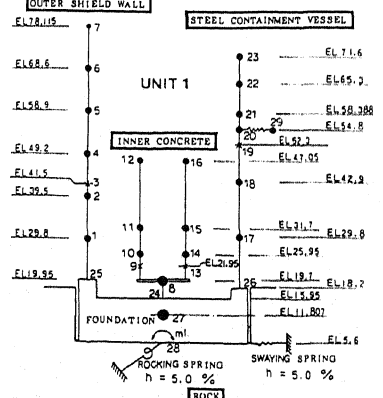


Fig. 15. ANALYTICAL MODEL. (1),(2)

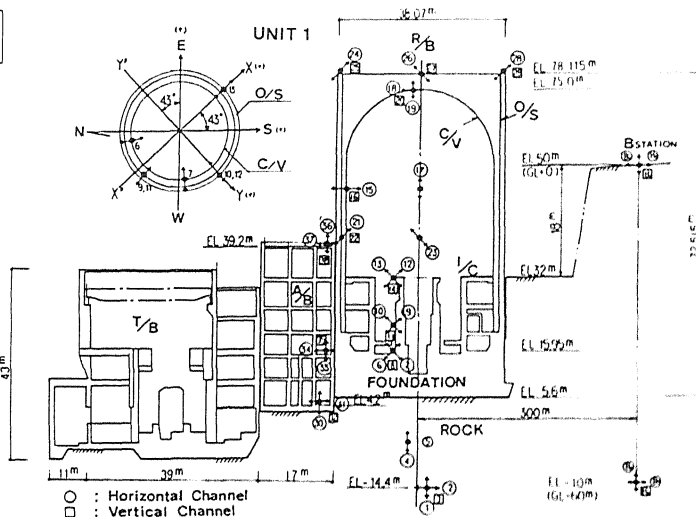


Fig. 12. LOCATION OF SEISMOGRAPH

Table IV. STATIC SWAY-ROCKING VALUE OF ROCK

| | SWAY SPRING | ROCKING SPRING |
|-------------------------------|--|---|
| DISTRIBUTION OF SOIL REACTION | UNIFORM DISTRIBUTION | TRIANGULAR DISTRIBUTION |
| SPRING VALUE | $K_{HS} = \frac{2 \pi \cdot G \cdot r}{2 - \nu}$ $= 1473 \times 10^6 \text{ t/m}$ | $K_{RS} = \frac{\pi \cdot G \cdot r^3}{2 (1 - \nu)}$ $= 3419 \times 10^6 \text{ t/m}^2 \cdot \text{rad}$ |
| REMARKS | r : RADIUS OF FOUNDATION (19035 m) G : MODULUS OF RIGIDITY OF ROCK (202 × 10^6 t/m^2) ν : POISSON'S RATIO OF ROCK (0.36) | |

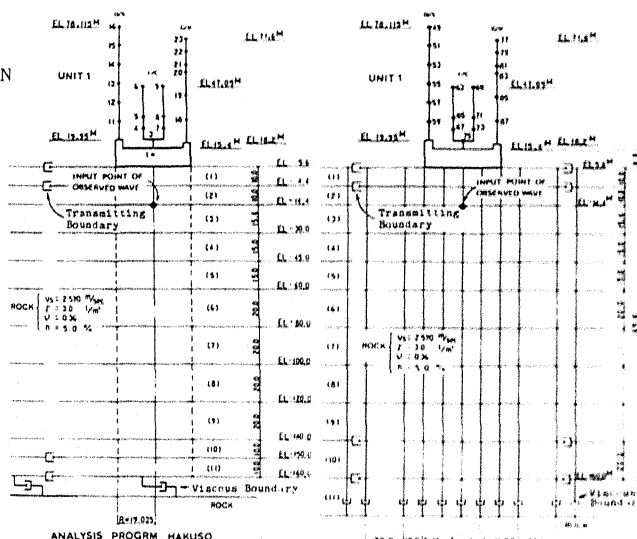


Fig. 16. ANALYTICAL MODEL. (3)

Fig. 17. ANALYTICAL MODEL. (4)

TABLE V COMPARISON OF THE FIRST-MODE FREQUENCIES

| STRUCTURE | FIRST-MODE FREQUENCY | EARTHQUAKE | SIMULATION ANALYSIS | DESIGN |
|--------------------------|----------------------|-----------------------|---------------------|--------|
| | | SUOH-NADA | | |
| OUTER SHIELD WALL | | 5.2 Hz (3.4~3.9) % | 5.18 Hz | 4.3 Hz |
| INNER CONCRETE | X-Dir | 9.8 (—) | 9.84 | 10.9 |
| | Y-Dir | 9.0 (3.9) | 8.96 | 9.6 |
| STEEL CONTAINMENT VESSEL | | 7.9~8.7 (1.6~1.7) | 7.86~8.42 | 7.1 |

NOTE: DAMPING FACTORS IN BRACKET ARE OBTAINED BY THE $1/2T$ METHOD

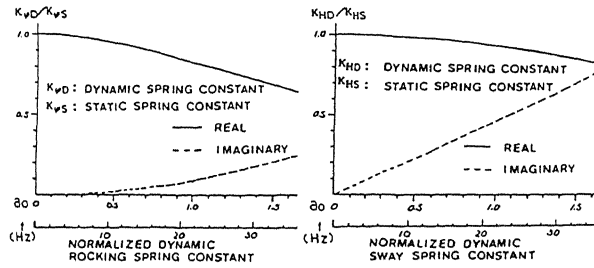


Fig. 18. NORMALIZED DYNAMIC SWAY-ROCKING SPRING.

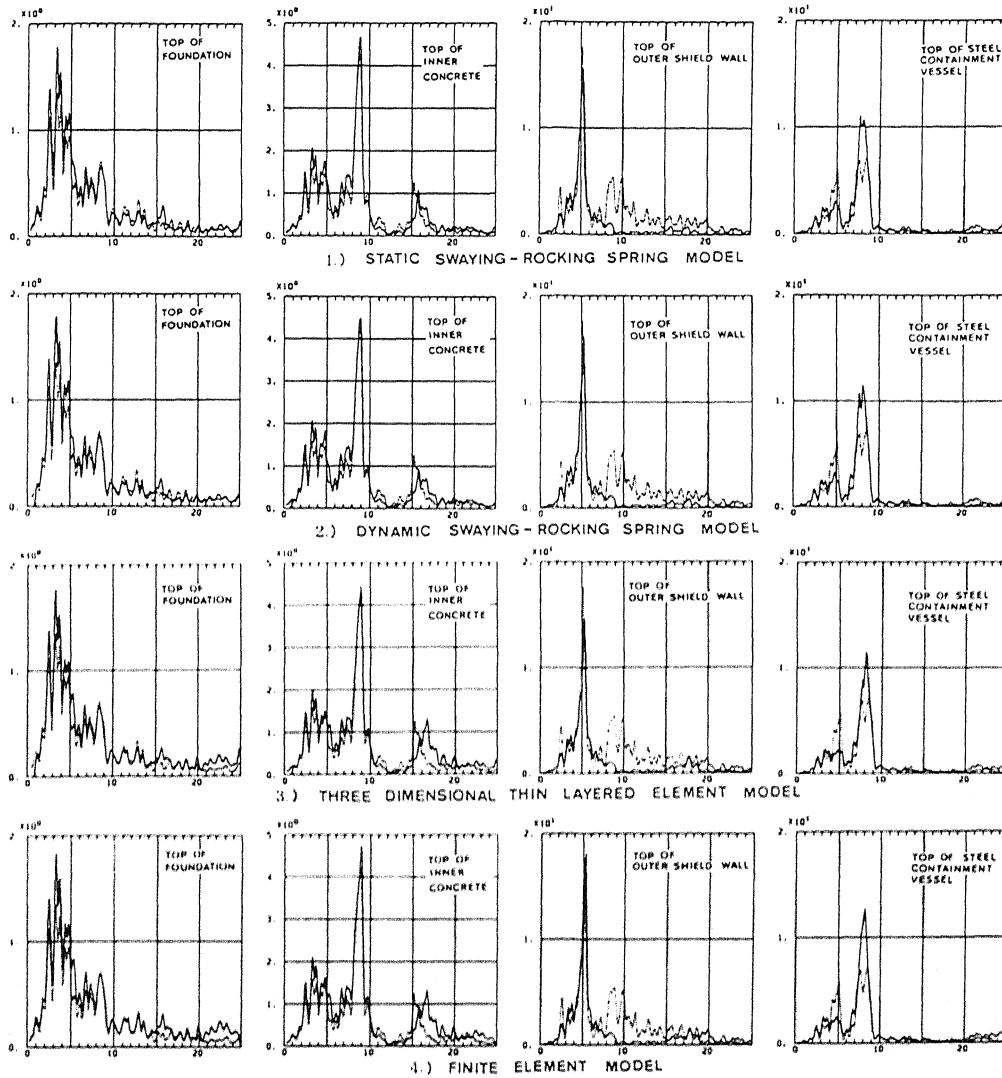


Fig. 20. COMPARISON OF SPECTRUMS OF OBSERVED AND ANALYZED WAVES

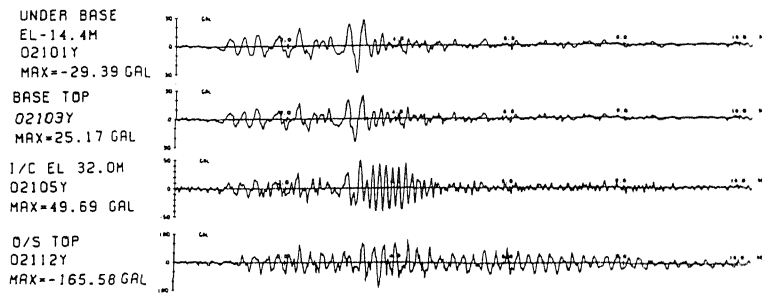


Fig. 13. OBSERVED WAVE (Y-DIR.)

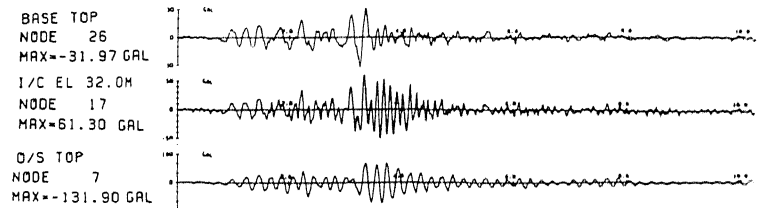


Fig. 21. ANALYZED WAVE BY 1) STATIC SPRING MODEL (Y-DIR.)

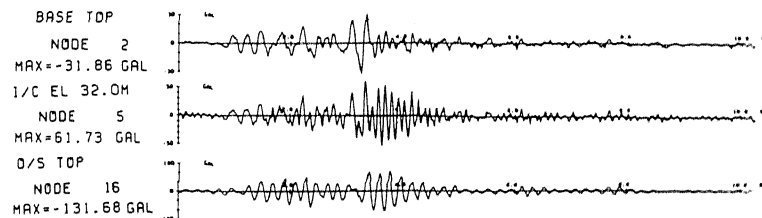


Fig. 22. ANALYZED WAVE BY 2) DYNAMIC SPRING MODEL (Y-DIR.)

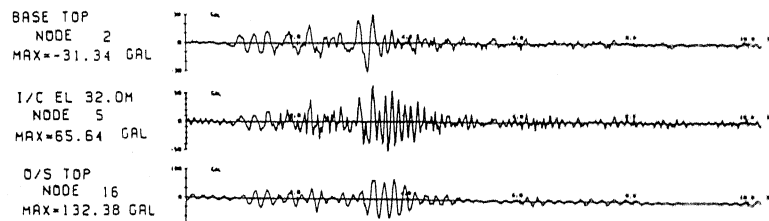


Fig. 23. ANALYZED WAVE BY 3) THIN LAYERED ELEMENT MODEL (Y-DIR.)

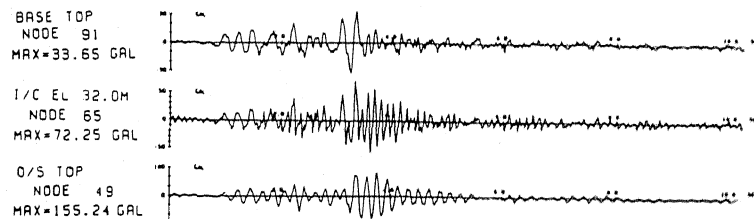


Fig. 24. ANALYZED WAVE BY 4) FINITE ELEMENT MODEL (Y-DIR.)